



QSAR modeling of VOCs degradation by ferrous-activated persulfate oxidation

Xin Zhu^a, Erdeng Du^b, Haoran Ding^a, Yusuo Lin^a, Tao Long^{a,*}, Huajie Li^b, Lei Wang^a

^aState Environmental Protection Key Laboratory of Soil Environmental Management and Pollution Control, Nanjing Institute of Environmental Sciences, Ministry of Environmental Protection of China, Nanjing 210042, China, emails: zhuxin@nies.org (X. Zhu), dinghr1989@sina.com (H. Ding), lys@nies.org (Y. Lin), Tel./Fax: +86 25 85287277; emails: longtao@nies.org (T. Long), leiwang@nies.org (L. Wang)

^bSchool of Environmental & Safety Engineering, Changzhou University, Changzhou 213164, China, emails: duerdeng@gmail.com (E. Du), lihuajie11@outlook.com (H. Li)

Received 2 December 2014; Accepted 6 May 2015

ABSTRACT

The objective of the study is to evaluate the degradability of volatile organic compounds (VOCs, in mixture) by sodium persulfate (SPS) with Fe(II) activation. Degradation of 51 VOCs by SPS alone and with 3 Fe(II)-based activators (i.e. ferrous ion, citric acid-chelated Fe(II), and EDTA-chelated Fe(II)) was investigated in batch experiments. In 48 h, 16 VOCs degraded over 90% with non-activated SPS, and 31 VOCs degraded over 90% with Fe(II) activation. The reaction rate constants of VOC degradation were also analyzed by quantitative structure-activity relationship (QSAR) model. Genetic algorithm and multiple linear regression analysis were applied to select the descriptors to build QSAR model. The main contribution to the degradation rate was given by energy level of highest occupied molecular orbital (E_{HOMO}), double bond equivalent, and the largest negative partial net charge on a carbon atom (Q_{c}^-). Based on cluster analysis of degradation rates and main descriptors, the degradability of target VOCs were classified into three classes—rapid, moderate, and slow. The obtained statistically robust QSAR model can be used to estimate the removal efficiency of VOCs by persulfate radicals.

Keywords: Persulfate oxidation; VOCs; QSAR model; Ferrous; Kinetics

1. Introduction

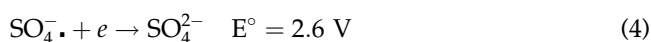
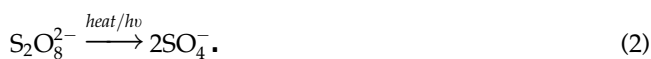
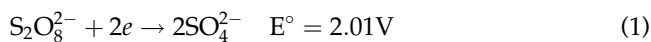
During the past three decades, substantial progress has been made to remediate soil and groundwater contaminated by volatile organic compounds (VOCs). Among various remediation technologies, *in situ* chemical oxidation (ISCO) has been widely applied due to its effectiveness and relative low cost [1–3]. Chemical oxidants that are traditionally used in ISCO

include Fenton's reagent, permanganate ($\text{KMnO}_4/\text{NaMnO}_4$), and ozone (O_3). Sodium persulfate ($\text{Na}_2\text{S}_2\text{O}_8$) is a relatively new oxidant applied in soil and groundwater remediation [4,5]. With the advantage of high solubility, good stability, and high reactivity with a wide range of contaminants, persulfate has become a favored oxidant in remediation projects [6]. Compared with traditional oxidants, persulfate shows less intensive damage to soil organic matter and indigenous microbial community, which may

*Corresponding author.

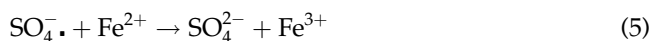
benefit the restoration of soil ecological functions after the treatment [7,8].

Persulfate ion ($S_2O_8^{2-}$), discovered by M. Berthelot in 1878, is a strong oxidant with a redox potential of 2.01 V, and can be thermally or chemically activated to generate sulfate radical ($SO_4^{\cdot-}$) [9,10].



Compared with persulfate itself, sulfate radical (Eq. (4)) is a stronger oxidant. The standard potential of sulfate radical is 2.6 V, close to that of hydroxyl radical (2.7 V) [11].

The initiator in Eq. (3) could be heat [12–14], transition metals (e.g. Fe, Cu, Ag, Ru, and Mn) [15–19], base [18,20,21], or hydrogen peroxide (H_2O_2) [22]. Among these initiators, ferrous ion is frequently used. The ferrous ion-activated persulfate reaction requires activation energy of 12 kcal mol^{-1} [23], which is lower than the value of $33.5 \text{ kcal mol}^{-1}$ required for thermal activation [10]. Studies have shown that iron-activated persulfate is an effective oxidant for degrading organic contaminants. Liang et al. [16] observed that sequential addition of Fe^{2+} in small increments resulted in an increased trichloroethylene (TCE) removal efficiency in the aqueous phase, which indicated Fe^{2+} played an important role in generating $SO_4^{\cdot-}$. However, they also found that excess Fe^{2+} would react with sulfate radicals as soon as they are generated, and the decontamination process would be inhibited (Eq. (5)).



Under neutral and basic pH, ferrous hydroxide is formed and precipitated from the aqueous solution, impairing the effectiveness of activation. To avoid the above mentioned issues, citric acid (CA)-chelated ferrous ion was adopted as activator, to control the concentration of free ferrous ion [24]. The availability of Fe^{2+} was controlled by adjusting the molar ratio of chelate/ Fe^{2+} . EDTA, EDDS, and hydroxylpropyl-beta-cyclodextrin (HPCD) were also proved to be applicative chelating agents for Fe^{2+} -activated SPS oxidation [25–28]. In this study, CA and EDTA were adopted as chelating agents in the oxidation system.

A wide range of VOCs have been detected in soil and groundwater at contaminated sites, while experimental data for estimating the treatability of individual compounds by activated SPS are still limited. Compared with the experimental analysis techniques, theoretical analysis, including quantitative structure-activity relationship (QSAR) method, could be used to investigate and assess the degradation of organic compounds with higher efficiency and lower cost [29,30].

The QSAR model is expected to reveal important structural feature (molecular descriptors) affecting the degradation of organic contaminants. Studies suggest that several chemical structure parameters may be critical to characterize the reaction activity of organic compounds with radicals, including O–H bond dissociation energy, highest occupied molecular orbital (HOMO) energy level (E_{HOMO}), and the relative adiabatic ionization potential [31,32]. These parameters are good theoretical indicators to predict reaction activity with radicals, and consequently correlate with the logarithm of the rate constant of organic compounds with radicals.

Several researchers have investigated the relationship between fate of VOCs and their inherent properties [33]. QSAR models were also developed to describe VOC degradation by tropospheric OH radicals [34] and NO_3 radicals [35], VOCs adsorption energies [36], and the inhalation toxicokinetics [37]. Till now, QSAR model for VOC degradation by sodium persulfate oxidation has not been reported. In this work, the reaction kinetics of VOCs with $Fe(II)$ -activated SPS was investigated. Experiments were designed to evaluate the effectiveness of SPS oxidation with $Fe(II)$ activation, and assess the degradability of targeted VOCs by SPS with different $Fe(II)$ -based activators (i.e. Fe^{2+} , CA-chelated Fe^{2+} and EDTA-chelated Fe^{2+}). The aim of this study is as follows: (a) to investigate the effect of different activation methods on SPS oxidation, (b) to establish the relationship between VOC degradation rate by SPS and molecular descriptors. The research could provide effective support for the control and management of VOCs contaminated sites treated by activated SPS.

2. Experimental

2.1. Materials and analysis

Sodium persulfate ($Na_2S_2O_8$), sulfuric acid (H_2SO_4), ferrous sulfate ($FeSO_4 \cdot 7H_2O$), CA, and EDTA were purchased from Sinopharm Chemical Reagent company, China. All chemicals were of analytical grade. Targeted VOCs (2 mg/mL solution standards in methanol, 54 components) were from J&K Chemical

Co. Ltd. Water used in this study was purified by a Millipore deionized water (DI) purification system.

Analysis of VOCs was conducted with the EPA SW-846 Method 8260C using a GC–MS system (Agilent 7890A/5975C) equipped with a capillary column (DB-624 60 m×0.25 mm×1.4 μm). The limit of quantification is 2 μg/L.

2.2. Batch experiments

The oxidation of VOCs was conducted under head-space free conditions in 43 mL glass vial reactors, and the concentration of Na₂S₂O₈ and Fe²⁺ were 5 g/L and 0.36 mmol/L, respectively. Typically, 37.5 mL of DI water, 5 mL of Na₂S₂O₈ stock solution (43 g/L), activator, and 50 μL VOC samples (200 μg/mL) were added to the glass vial, and the total volume was adjusted to 43 mL. The concentration of each component in the VOC mixture was approximately 250 μg/L. Four sets of experiments were carried out, where non-activated SPS was used in Experiment 1 and Fe(II)-activated SPS were used in Experiments 2–4. The pH of Experiment 2 was 2.62 while others were under neutral pH. The molar ratio of chelating agent and Fe²⁺ was 1:5 in both CA and EDTA experiments. Detailed parameters of each experiment are shown in Table 1. Samples were prepared in triplicate for each of the experiment and analyzed at different reaction time (0, 6, 12, 24, and 48 h). Control samples were also prepared in triplicate to provide baseline values. Compounds showed over 20% of loss in total mass after 48 h in the control samples would be excluded from further analysis.

Solution of mixed VOCs was used in this study. The concentration of each VOC was relatively low compared with that of persulfate (250 μg/L vs. 5 g/L), thus the reaction rate was not limited by radical concentration, and the competition of VOC species for radical became negligible. Huang et al. [13] used a similar system to study thermally activated SPS oxidation, and found some VOCs showed negative degradation under 1 g/L SPS oxidation, indicating intermediates of decomposition could be formed.

However, this phenomenon was less pronounced when the SPS concentration increased to 5 g/L.

2.3. Calculation of molecular descriptors

In this work, 51 VOCs were selected to investigate the relationship of persulfate oxidation rate and molecular descriptors. Density functional theory (DFT) was usually considered fairly accurate to optimize the geometric structure of organic compounds. Therefore, 51 VOCs were optimized by DFT/B3LYP method on the basis set of 6-31+g(d,p) to obtain the static parameters. Vibration frequency analysis showed that there was no virtual frequency for the optimized structure, which corresponds to the minimum points on potential energy surface. The calculation process was performed by Gaussian 09 program [38].

Total of 13 theoretical molecular descriptors were selected for the preliminary model development (Table 2), including double bond equivalent (DBE), the largest negative partial net charge on a carbon atom (Q_c^-), the largest positive net charge on a hydrogen atom (Q_h^+), total energy (TE), surface area (SAG), molecular volume, hydration energy (HE), partition coefficient (Log *P*), refractivity (*R*), energy of the highest occupied molecular orbital (E_{HOMO}), energy of the lowest unoccupied molecular orbital (E_{LUMO}), and dipole moment (μ).

2.4. QSAR model analysis

Build QSAR [39] program was used to build the QSAR models. The genetic algorithm (GA) method and multiple linear regression (MLR) were adopted to select the optimal combinations of descriptors for QSAR models. The combination of the genetic algorithm and multiple linear regression analysis (GA-MLR) techniques was successfully applied to find the best descriptors and to construct several QSAE models [29,40,41]. GA method is an optimization algorithm, which is used to search for the best model in terms of the highest correlation coefficient and the lowest standard deviation equations [39]. The control

Table 1

List of experiments conducted for the degradation of VOCs with activated SPS oxidation

Experiment	Na ₂ S ₂ O ₈ (g/L)	Fe ²⁺ (mM)	CA (mM)	EDTA (mM)
1	5	0	0	0
2	5	0.36	0	0
3	5	0.36	0.072	0
4	5	0.36	0	0.072

Table 2
Structural descriptors of 51 VOCs

No.	Compounds name	CAS	DBE	E_{HOMO} (eV)	E_{LUMO} (eV)	Q_c^- (e)	Q_h^+ (e)	μ	TE	SAG (\AA^2)	Volume (\AA^3)	Hydration energy	Log P	R	Polarizability
1	1,1-Dichloroethene	75-35-4	1	-7.253	-0.474	-0.191	0.142	1.510	-997.8	216.5	290.0	-1.95	1.820	20.460	8.110
2	Methylene Chloride	75-09-2	0	-8.419	-0.435	-0.366	0.205	1.850	-959.7	200.4	254.6	1.48	1.150	16.440	6.470
3	trans-1,2-Dichloroethylene	156-60-5	1	-7.077	-0.539	-0.169	0.168	0.000	-997.8	224.2	292.4	-0.92	0.890	19.640	8.110
4	1,1-Dichloroethane	75-34-3	0	-8.280	-0.333	-0.300	0.151	2.275	-999.0	228.5	306.3	2.95	1.160	21.280	8.300
5	cis-1,2-Dichloroethylene	156-59-2	1	-7.073	-0.417	-0.178	0.161	2.044	-997.8	219.4	290.0	-0.92	0.890	19.640	8.110
6	Bromochloromethane	74-97-5	0	-7.878	-0.859	-0.302	0.199	1.700	-3071.2	211.0	274.8	1.48	1.030	19.250	7.160
7	Chloroform	67-66-3	0	-8.598	-1.357	-0.358	0.241	1.274	-1419.3	225.1	398.7	1.48	1.610	21.360	8.390
8	1,2-Dichloroethane	107-06-2	0	-8.351	-0.173	-0.276	0.177	0.000	-999.0	232.0	309.1	2.95	1.590	20.660	8.300
9	1,1,1-Trichloroethane	71-55-6	0	-8.385	-1.230	-0.284	0.155	2.006	-1458.6	249.8	347.2	1.50	2.040	26.220	10.230
10	1,1-Dichloropropene	563-58-6	1	-6.852	-0.150	-0.357	0.138	2.128	-1037.1	250.1	341.6	-0.14	2.180	26.130	9.940
11	Carbon chloride	56-23-5	0	-8.833	-2.119	-0.358	0.000	0.001	-1878.9	248.1	340.6	0.04	3.370	26.850	10.320
12	Benzene	71-43-2	4	-6.719	0.073	-0.084	0.084	0.000	-232.3	237.4	329.9	-2.11	2.050	26.060	10.430
13	Dibromomethane	74-95-3	1	-7.667	-1.076	-0.227	0.193	1.547	-5182.7	219.6	294.2	1.48	0.910	22.070	7.860
14	1,2-Dichloropropane	78-87-5	0	-8.216	-0.203	-0.304	0.176	0.618	-1038.3	254.5	356.5	4.43	2.000	25.070	10.140
15	Trichloroethylene	79-01-6	1	-7.114	-0.811	-0.172	0.178	0.949	-1457.4	246.6	333.9	-1.67	1.710	25.290	10.040
16	Dichlorobromomethane	124-48-1	0	-8.088	-1.665	-0.297	0.235	1.171	-3530.8	234.3	318.1	1.48	1.580	24.170	9.090
17	cis-1,3-Dichloropropene	10061-01-5	1	-7.073	-0.417	-0.178	0.161	2.044	-997.8	219.4	290.0	-0.92	0.890	19.640	8.110
18	trans-1,3-Dichloropropene	10061-02-6	1	-7.153	-0.465	-0.320	0.175	1.859	-1037.1	257.6	349.4	0.71	1.510	25.310	9.940
19	1,1,2-Trichloroethane	79-00-5	0	-8.473	-0.737	-0.271	0.217	1.384	-1458.6	253.8	350.8	2.95	1.820	25.710	10.230
20	Toluene	108-88-3	4	-6.411	0.081	-0.381	0.122	0.344	-271.6	268.4	384.2	-1.39	2.510	31.100	12.270
21	1,3-Dichloropropane	142-28-9	0	-8.056	-0.236	-0.296	0.158	2.035	-1038.3	264.2	364.4	4.43	1.640	25.520	10.140
22	Dibromochloromethane	124-48-1	0	-7.821	-1.851	-0.226	0.228	1.064	-5642.3	243.8	337.4	1.48	1.550	26.980	9.790
23	1,2-Dibromoethane	106-93-4	0	-7.677	-0.876	-0.201	0.170	0.000	-5222.0	250.1	348.1	2.95	1.710	26.620	9.700
24	Tetrachloroethylene	127-18-4	1	-7.117	-1.095	-0.175	0.000	0.000	-1916.9	264.7	374.3	-2.53	2.520	30.950	11.960
25	1,1,2,2-Tetrachloroethane	79-34-5	0	-8.657	-0.987	-0.267	0.223	1.904	-1918.2	273.9	390.3	2.95	2.060	30.760	12.160
26	Chlorobenzene	108-90-7	4	-6.714	-0.365	-0.093	0.110	1.918	-691.9	264.5	376.1	-2.90	2.560	30.860	12.360
27	Ethylbenzene	100-41-4	4	-6.372	0.098	-0.328	0.112	0.459	-310.9	290.3	432.7	0.19	2.910	35.700	14.100
28	p-Xylene & m-Xylene	106-42-3	4	-6.142	0.173	-0.381	0.120	0.096	-310.9	297.3	436.9	-0.72	2.980	36.140	14.100
29	Bromoform	75-25-2	0	-7.649	-1.999	-0.143	0.221	0.951	-7753.8	253.9	355.1	1.48	1.520	29.790	10.490
30	Styrene	100-42-5	5	-6.047	-0.853	-0.252	0.101	0.187	-309.7	283.5	416.0	-3.73	2.700	35.740	13.910
31	o-Xylene	95-47-6	4	-6.248	0.195	-0.381	0.118	0.585	-310.9	286.3	427.8	-0.77	2.980	36.140	14.100
32	1,2,3-Trichloropropane	96-18-4	0	-8.294	-0.462	-0.271	0.163	1.631	-1497.9	275.4	397.0	4.43	2.360	29.670	12.060

(Continued)

Table 2 (Continued)

No.	Compounds name	CAS	DBE	E_{HOMO} (eV)	E_{LUMO} (eV)	Q_{c}^{-} (e)	Q_{h}^{+} (e)	μ	TE	SAG (\AA^2)	Volume (\AA^3)	Hydration energy	Log P	R	Polarizability
33	Isopropyl benzene	98-82-8	4	-6.425	0.098	-0.304	0.107	0.284	-350.2	320.8	480.8	1.77	3.240	40.250	15.940
34	Bromobenzene	108-86-1	4	-6.590	-0.366	-0.086	0.109	1.810	-2803.4	274.7	394.7	-2.89	2.840	33.680	13.060
35	n-Propylbenzene	103-65-1	4	-6.408	0.123	-0.317	0.103	0.325	-350.2	323.7	490.0	1.71	3.310	40.300	15.940
36	2-Chlorotoluene	95-49-8	4	-6.568	-0.265	-0.378	0.136	1.665	-731.2	285.2	422.3	-2.27	3.030	35.900	14.200
37	p-Chlorotoluene	106-43-4	4	-6.455	-0.333	-0.382	0.126	2.350	-731.2	292.6	429.4	-2.22	3.030	35.900	14.200
38	1,3,5-Trimethylbenzene	108-67-8	4	-6.148	0.154	-0.381	0.120	0.088	-350.2	322.6	489.8	-0.12	3.450	41.180	15.940
39	tert-Butylbenzene	98-06-6	4	-6.412	0.101	-0.310	0.105	0.325	-389.5	332.3	518.8	1.87	3.670	44.720	17.770
40	1,2,4-Trimethylbenzene	95-63-6	4	-6.014	0.203	-0.382	0.119	0.290	-350.2	315.0	480.6	-0.15	3.450	41.180	15.940
41	4-Propyltoluene	1074-55-1	4	-6.143	0.133	-0.381	0.122	0.134	-389.5	350.4	543.3	2.35	3.770	45.340	17.770
42	1,4-Dichlorobenzene	106-46-7	4	-6.750	-0.764	-0.094	0.120	0.000	-1151.4	288.2	421.1	-3.72	3.080	35.670	14.290
43	1,3-Dichlorobenzene	541-73-1	4	-6.927	-0.742	-0.094	0.133	1.797	-1151.4	289.2	420.3	-3.73	3.080	35.670	14.290
44	p-Isopropyltoluene	99-87-6	4	-6.156	0.100	-0.381	0.121	0.092	-389.5	349.0	533.5	2.40	3.710	45.290	17.770
45	1,2-Dichlorobenzene	95-50-1	4	-6.848	-0.673	-0.088	0.118	2.761	-1151.4	285.2	416.4	-3.76	3.080	35.670	14.290
46	n-Butylbenzene	104-51-8	4	-6.397	0.125	-0.318	0.103	0.361	-389.5	360.3	545.7	3.19	3.700	44.900	17.770
47	1,2-Dibromo-3-chloro- propane	96-12-8	0	-7.533	-0.983	-0.278	0.190	1.403	-5721.0	292.6	431.5	4.43	2.490	35.640	13.460
48	1,2,4-Trichlorobenzene	120-82-1	4	-6.926	-1.037	-0.093	0.139	1.401	-1611.0	310.0	460.7	-4.63	3.600	40.470	16.220
49	Naphthalene	91-20-3	7	-5.803	-0.979	-0.129	0.085	0.000	-385.9	302.8	457.8	-4.76	3.050	42.510	17.700
50	Hexachlorobutadiene	87-68-3	2	-6.733	-2.375	-0.240	0.000	0.000	-2913.5	344.9	527.7	-5.07	2.610	50.700	19.300
51	1,2,3-Trichlorobenzene	87-61-6	4	-7.100	-0.955	-0.086	0.122	2.800	-1611.0	307.0	455.9	-4.67	3.600	40.470	16.220

Notes: DBE (double bond equivalent), E_{HOMO} (energy of the highest occupied molecular orbital), Q_{c}^{-} (the largest negative partial net charge on a carbon atom), Q_{h}^{+} (the largest positive net charge on a hydrogen atom), μ (dipole moment), TE (total energy), SAG (surface area), Log P (partition coefficient), R (refractivity).

parameters were as follows: total variables in models ranging from 1 to 4, the number of models per generation 30, mutation probability 35%, the number of generation 200 [30]. The data-set of 51 compounds was divided into two groups: 46 compounds were used as training set to develop the models, and five compounds were used as test set for external validation.

3. Results and discussion

3.1. Degradability of VOCs by persulfate oxidation

Table 3 shows the results of VOC degradation by SPS over time. Most of the VOCs could be degraded by SPS of 5 g/L. At room temperature (20°C), 35 of the 51 VOCs degraded over 25% after 48 h. The ratio of degradation increased with reaction time. The concentration of VOCs changed little in the first 6 h. Degradation of some VOCs was observed after 12 h. After 48 h, 16 VOCs degraded over 90%. However, no obvious degradation was observed on most alkanes.

Table 4 shows the results of VOC degradation by Fe²⁺-activated sodium persulfate (SPS-Fe(II)) over time. Most of the VOCs showed elevated degradation efficiency compared with the reaction with inactivated SPS, which confirmed the enhancement of SPS oxidizing capacity with Fe²⁺ activation. For dibromochloromethane, bromoform, 1,2,3-trichloro-propane, 1,1,2,2-tetrachloroethane, and 1,2-dibromo-3-chloropropane, significant differences of degradation were observed between SPS treatment and SPS-Fe(II) treatment. After 48 h reaction, 40 of the 51 VOCs had a percentage of degradation over 25%, 31 VOCs degraded over 90%.

The results above demonstrated that Fe²⁺-activated SPS could effectively degrade the targeted VOCs. However, excess Fe²⁺ in solution would act as scavengers of sulfate free radicals (Eq. (5)) and adversely affect the effectiveness of oxidation. To control the presence of excess Fe²⁺, chelating agents CA and EDTA were added, respectively, and the molar ratio of Fe²⁺ to CA/EDTA used in this study was 1: 5. Table 5 shows the results of VOC degradation with SPS, SPS-Fe(II), SPS-Fe(II)/CA, and SPS-Fe(II)/EDTA in 12 h. Assessed by the overall removal of VOCs, systems activated with chelated ferrous ion demonstrated improved reactivity.

3.2. Kinetic parameters of degradation of VOCs

The degradation of VOCs was usually reported to follow pseudo-second-order kinetics [20,42,43], as follows:

$$\frac{1}{C_t} = 1 + k_{\text{obs}}C_0t \quad (6)$$

where k_{obs} is the second-order rate constant, t is reaction time, C_0 and C_t are the concentration of reactant at time zero and t , respectively. Data from batch degradation experiments of VOCs by various oxidants were fitted with Eq. (6), and the results are shown in Table 6. As can be seen, the degradation of most VOCs by SPS was fitted well with the second-order model. Activated SPS exhibited stronger oxidation capacity with much larger rate constant than its inactivated state. Degradation of most VOCs yielded highest rate constant with Fe(II)/CA as the activator, followed by Fe(II)/EDTA, which indicated that chelating agents could increase the stability and solubility of ferrous ion as well as the reaction efficiency of the system.

The experimental results demonstrated that activation of SPS can significantly improve the degradation rate of certain VOCs. For example, the degradation rate constants of 1,3,5-trimethylbenzene by the activation methods of ferrous ion, Fe(II)/CA, Fe(II)/EDTA are 0.4096, 3.182, 0.523 L μg⁻¹ h⁻¹, respectively. Compared to the rate (0.0045 L μg⁻¹ h⁻¹) by SPS oxidation alone, the rates by three enhanced activation methods are significantly improved by 91, 707, and 116 times.

3.3. QSAR model of VOC degradation by ferrous-activated persulfate oxidation

The logarithm of rate constants of VOC degradation by SPS-Fe(II) (Log k) was taken to build QSAR model. GA-MLR was applied to select the relative optimal MLR regression model, as shown in Table 7. Results indicated that the regression coefficients of MLR model no longer increase when the number of descriptors is over three. Therefore, three-variable MLR model is taken as the optimized model with E_{HOMO} , DBE, and Q_c^- as descriptors.

$$-\log k = -1.571E_{\text{HOMO}} + 2.605Q_c^- - 0.131\text{DBE} - 7.717 \quad (7)$$

Table 7 also shows that, E_{HOMO} , one of the most important quantum chemical descriptors, has a major contribution to VOC degradation in 1-, 2-, 3-variable models. The value of E_{HOMO} positively correlates with the degradation rate of VOCs. The energies of frontier molecular orbitals, including E_{HOMO} , E_{LUMO} , E_{GAP} , has successfully applied to the construction of many

Table 3
Degradation of 51 VOCs over time with SPS

Compound	Concentration of VOCs ($\mu\text{g/L}$)					% Degradation at 48 h
	0	6	12	24	48	
1,1-Dichloroethene	269	241	177	100	57	78.9
Methylene Chloride	261	261	237	219	213	18.1
trans-1,2-Dichloroethylene	265	255	209	157	123	53.7
1,1-Dichloroethane	255	261	236	227	220	13.6
cis-1,2-Dichloroethylene	249	242	198	149	117	53.2
Bromochloromethane	256	260	236	220	215	16.3
Chloroform	246	252	229	218	213	13.5
1,2-Dichloroethane	247	252	227	207	202	18.3
1,1,1-Trichloroethane	252	263	233	219	212	15.6
1,1-Dichloropropene	248	201	121	50	15	93.9
Carbon chloride	251	262	233	215	207	17.5
Benzene	246	217	149	75	35	85.7
Dibromomethane	265	279	259	240	232	12.3
1,2-Dichloropropane	252	267	240	226	219	12.9
Trichloroethylene	253	239	187	125	86	66.1
Dichlorobromomethane	248	256	233	219	212	14.6
cis-1,3-Dichloropropene	240	236	194	139	101	57.8
trans-1,3-Dichloropropene	238	234	191	130	93	61.1
1,1,2-Trichloroethane	247	263	242	219	208	16.0
Toluene	256	203	114	42	9	96.4
1,3-Dichloropropane	241	253	234	209	197	18.5
Dibromochloromethane	250	262	242	215	202	19.0
1,2-Dibromoethane	249	263	243	214	202	18.9
Tetrachloroethylene	260	247	196	130	90	65.4
1,1,2,2-Tetrachloroethane	258	275	258	203	188	27.4
Chlorobenzene	248	225	164	86	46	81.5
Ethylbenzene	245	200	119	44	12	95.3
p-Xylene & m-Xylene	488	368	196	62	10	97.7
Bromoform	248	263	244	201	187	24.5
Styrene	244	144	51	9	ND	99.7
o-Xylene	244	186	99	31	5	97.8
1,2,3-Trichloro-propane	230	245	229	183	173	25.1
Isopropyl benzene	242	202	126	50	16	93.6
Bromobenzene	237	207	144	67	31	86.8
n-Propylbenzene	239	194	118	44	13	94.6
2-Chlorotoluene	238	190	111	39	10	96.0
p-Chlorotoluene	520	361	167	46	9	98.3
1,3,5-Trimethylbenzene	239	179	93	28	5	98.1
tert-Butylbenzene	246	201	125	54	18	92.5
1,2,4-Trimethylbenzene	238	179	96	30	5	97.7
p-Propyl-toluene	239	199	127	52	18	92.4
1,4-Dichlorobenzene	247	237	188	120	88	64.2
1,3-Dichlorobenzene	248	227	170	90	53	78.5
p-Isopropyltoluene	241	188	109	38	11	95.4
1,2-Dichlorobenzene	245	234	190	117	84	65.6
n-Butylbenzene	232	186	112	41	13	94.6
1,2-Dibromo-3-chloro-propane	245	260	248	191	175	28.7
1,2,4-Trichlorobenzene	237	232	192	109	76	67.7
Naphthalene	248	205	139	60	34	86.2
Hexachlorobutadiene	227	232	216	197	183	19.5
1,2,3-Trichlorobenzene	256	273	244	174	151	40.9

Notes: The reported data are the averages of three replicate experiments.

The data $>2 \mu\text{g/L}$ are used to determine the degradation rate.

ND $<2 \mu\text{g/L}$ (practical quantification limit).

Table 4
Degradation of 51VOCs over time with Fe(II)-activated SPS

Compound	Concentration of VOCs ($\mu\text{g/L}$)					% Degradation at 48 h
	0	6	12	24	48	
1,1-Dichloroethene	269	200	138	25	ND	99.6
Methylene Chloride	261	226	241	209	222	14.8
trans-1,2-Dichloroethylene	265	213	187	83	8	97.1
1,1-Dichloroethane	255	221	237	213	223	12.8
cis-1,2-Dichloroethylene	249	203	179	94	23	90.7
Bromochloromethane	256	224	239	200	214	16.4
Chloroform	246	215	230	201	214	13.1
1,2-Dichloroethane	247	214	228	183	200	19.2
1,1,1-Trichloroethane	252	225	236	209	209	16.8
1,1-Dichloropropene	248	155	68	2	ND	100.0
Carbon chloride	251	225	236	203	198	21.2
Benzene	246	167	99	11	ND	99.9
Dibromomethane	265	222	252	207	222	16.2
1,2-dichloropropane	252	215	236	203	214	15.2
Trichloroethylene	253	193	154	52	2	99.2
Dichlorobromomethane	248	216	232	198	199	19.9
cis-1,3-Dichloropropene	240	193	169	74	7	96.9
trans-1,3-Dichloropropene	238	187	167	63	6	97.5
1,1,2-Trichloroethane	247	209	235	179	189	23.5
Toluene	256	148	57	ND	ND	100.0
1,3-Dichloropropane	241	206	228	171	181	25.0
Dibromochloromethane	250	214	235	173	165	33.8
1,2-Dibromoethane	249	204	233	170	182	26.7
Tetrachloroethylene	260	198	160	55	3	98.7
1,1,2,2-Tetrachloroethane	258	214	239	149	165	36.4
Chlorobenzene	248	169	113	16	ND	100.0
Ethylbenzene	245	147	63	2	ND	100.0
p-Xylene & m-Xylene	488	266	88	ND	ND	100.0
Bromoform	248	208	231	152	140	43.4
Styrene	244	79	7	ND	ND	100.0
o-Xylene	244	133	43	ND	ND	100.0
1,2,3-Trichloro-propane	230	194	216	143	148	36.0
Isopropyl benzene	242	150	70	3	ND	100.0
Bromobenzene	237	160	95	9	ND	100.0
n-Propylbenzene	239	146	64	2	ND	99.9
2-Chlorotoluene	238	141	56	ND	ND	99.9
p-Chlorotoluene	520	230	68	ND	ND	100.0
1,3,5-Trimethylbenzene	239	127	38	ND	ND	100.0
tert-Butylbenzene	246	155	72	4	ND	100.0
1,2,4-Trimethylbenzene	238	128	41	ND	ND	100.0
p-Propyl-toluene	239	152	74	4	ND	99.9
1,4-Dichlorobenzene	247	184	148	48	3	98.8
1,3-Dichlorobenzene	248	175	122	22	ND	99.9
p-Isopropyltoluene	241	138	54	3	2	99.3
1,2-Dichlorobenzene	245	181	147	44	3	98.9
n-Butylbenzene	232	142	60	2	ND	99.9
1,2-Dibromo-3-chloro-propane	245	199	227	128	140	42.9
1,2,4-Trichlorobenzene	237	178	148	37	5	98.1
Naphthalene	248	140	71	3	4	98.5
Hexachlorobutadiene	227	212	209	179	161	29.3
1,2,3-Trichlorobenzene	256	214	210	90	54	79.1

Notes: The reported data are the averages of three replicate experiments.

The data $>2 \mu\text{g/L}$ are used to determine the degradation rate.

ND $<2 \mu\text{g/L}$ (practical quantification limit).

Table 5
Summary of degradation of VOCs by SPS under different activation conditions

Compound	% Degradation at 12 h				% Degradation at 48 h with SPS-Fe(II)/CA
	SPS	SPS-Fe(II)	SPS-Fe(II)/CA	SPS-Fe(II)/EDTA	
1,1-Dichloroethene	34.0	48.6	74.1	63.5	99.7
Methylene Chloride	9.2	7.5	9.5	17.7	29.2
trans-1,2-Dichloroethylene	20.9	29.5	47.4	41.3	99.2
1,1-Dichloroethane	7.7	7.1	3.2	11.8	14.6
cis-1,2-Dichloroethylene	20.6	28.2	42.0	39.3	100.0
Bromochloromethane	7.9	6.9	7.5	14.2	22.8
Chloroform	6.8	6.4	5.0	12.2	19.5
1,2-Dichloroethane	8.3	7.9	8.9	15.0	21.9
1,1,1-Trichloroethane	7.5	6.3	7.5	16.5	21.4
1,1-Dichloropropene	51.3	72.4	93.0	83.8	100.0
Carbon chloride	7.4	6.1	9.5	17.2	24.5
Benzene	39.7	59.9	83.4	72.1	99.9
Dibromomethane	2.3	5.0	3.1	10.5	30.2
1,2-dichloropropane	4.6	6.2	2.8	11.7	21.2
Trichloroethylene	26.1	39.1	61.0	51.2	99.8
Dichlorobromomethane	6.1	6.7	6.8	13.2	29.2
cis-1,3-Dichloropropene	19.4	29.7	45.8	39.6	98.5
trans-1,3-Dichloropropene	19.9	30.0	47.9	40.8	98.8
1,1,2-Trichloroethane	2.0	4.9	3.6	10.2	29.1
Toluene	55.6	77.9	95.8	88.1	100.0
1,3-Dichloropropane	2.9	5.7	6.5	11.0	31.0
Dibromochloromethane	2.9	5.9	9.8	13.8	44.1
1,2-Dibromoethane	2.3	6.4	6.5	12.0	35.2
Tetrachloroethylene	24.6	38.7	59.8	50.8	99.5
1,1,2,2-Tetrachloroethane	0.1	7.4	11.5	16.3	37.5
Chlorobenzene	33.9	54.6	78.8	67.1	99.9
Ethylbenzene	51.5	74.2	94.3	85.6	100.0
p-Xylene & m-Xylene	59.9	82.1	97.6	91.5	100.0
Bromoform	1.7	6.9	13.4	16.0	49.0
Styrene	79.0	97.3	99.9	99.4	100.0
o-Xylene	59.4	82.2	97.5	91.7	100.0
1,2,3-Trichloro-propane	0.8	6.4	11.6	15.2	33.2
Isopropyl benzene	48.0	71.0	92.6	83.0	100.0
Bromobenzene	39.1	59.9	84.7	73.4	100.0
n-Propylbenzene	50.7	73.3	93.8	84.9	100.0
2-Chlorotoluene	53.4	76.3	95.2	87.3	100.0
p-Chlorotoluene	67.9	86.9	98.0	93.9	100.0
1,3,5-Trimethylbenzene	61.1	84.1	98.1	93.0	100.0
tert-Butylbenzene	49.1	70.6	91.4	82.0	100.0
1,2,4-Trimethylbenzene	59.7	82.7	97.8	92.1	100.0
p-Propyl-toluene	46.9	69.1	91.3	81.5	100.0
1,4-Dichlorobenzene	23.9	39.9	60.8	52.0	99.6
1,3-Dichlorobenzene	31.5	50.7	74.4	63.7	100.0
p-Isopropyltoluene	54.8	77.8	95.2	88.3	99.0
1,2-Dichlorobenzene	22.5	40.0	62.2	52.8	99.7
n-Butylbenzene	51.8	74.1	94.1	85.6	100.0
1,2-Dibromo-3-chloro-propane	–	7.4	14.0	14.6	40.5
1,2,4-Trichlorobenzene	19.0	37.5	60.8	48.9	99.4
Naphthalene	44.2	71.5	91.4	82.8	100.0
Hexachlorobutadiene	4.7	7.9	13.0	14.9	33.3
1,2,3-Trichlorobenzene	4.8	17.9	33.8	25.1	84.8

Note: “–” no degradation was observed.

Table 6
The VOCs degradation rate constant (k) by SPS under different reaction conditions

Compound Name	SPS		SPS-Fe(II)		SPS-Fe(II)/CA		SPS-Fe(II)/EDTA	
	k (L μg^{-1} h $^{-1}$)	R^2	k (L μg^{-1} h $^{-1}$)	R^2	k (L μg^{-1} h $^{-1}$)	R^2	k (L μg^{-1} h $^{-1}$)	R^2
1,1-Dichloroethene	3.05E-04	0.98	0.02058	0.74	0.02539	0.82	0.02728	0.77
Methylene Chloride	1.91E-05	0.78	1.17E-05	0.16	2.85E-05	0.80	3.81E-05	0.95
trans-1,2-Dichloroethylene	9.68E-05	0.97	0.00264	0.77	0.00948	0.75	0.00704	0.75
1,1-Dichloroethane	1.43E-05	0.71	8.94E-06	0.08	1.18E-05	0.71	2.85E-05	0.98
cis-1,2-Dichloroethylene	1.01E-04	0.97	8.26E-04	0.85	4.39E-04	0.92	0.00549	0.74
Bromochloromethane	1.77E-05	0.94	1.45E-05	0.92	2.05E-05	0.89	2.84E-05	0.94
Chloroform	1.50E-05	0.75	1.06E-05	0.24	1.77E-05	0.80	2.94E-05	0.97
1,2-Dichloroethane	2.12E-05	0.73	1.93E-05	0.11	1.97E-05	0.79	3.28E-05	0.95
1,1,1-Trichloroethane	1.79E-05	0.76	1.50E-05	0.26	1.75E-05	0.79	3.24E-05	0.92
1,1-Dichloropropene	0.00134	0.70	0.81981	0.55	0.28133	0.57	0.0801	0.67
Carbon chloride(CCl4)	2.05E-05	0.91	2.13E-05	0.72	2.17E-05	0.67	3.56E-05	0.94
Benzene	5.30E-04	0.76	0.1175	0.73	0.06986	0.70	0.07311	0.77
Dibromomethane	1.38E-05	0.97	1.26E-05	0.72	3.30E-05	0.84	3.83E-05	0.99
1,2-Dichloropropane	1.53E-05	0.74	1.20E-05	0.08	2.06E-05	0.88	3.14E-05	0.98
Trichloroethylene	1.70E-04	0.69	0.01096	0.14	0.0344	0.84	0.01701	0.74
Dichlorobromomethane	1.66E-05	0.98	1.90E-05	0.74	3.24E-05	0.73	3.90E-05	0.99
cis-1,3-Dichloropropene	1.26E-04	0.78	0.00276	0.53	0.00571	0.90	0.00375	0.78
trans-1,3-Dichloropropene	1.47E-04	0.98	0.00345	0.77	0.00732	0.77	0.00453	0.77
1,1,2-Trichloroethane	1.99E-05	0.98	2.53E-05	0.77	3.29E-05	0.76	3.96E-05	0.99
Toluene	0.00225	0.79	4.0361	0.38	2.90454	0.87	0.20654	0.66
1,3-Dichloropropane	2.33E-05	0.87	2.89E-05	0.71	3.62E-05	0.81	3.98E-05	1.00
Dibromochloromethane	2.33E-05	0.85	4.34E-05	0.42	6.27E-05	0.87	6.22E-05	0.99
1,2-Dibromoethane	2.37E-05	0.84	2.99E-05	0.74	4.26E-05	0.89	4.77E-05	0.99
Tetrachloroethylene	1.60E-04	0.82	0.00625	0.36	0.01717	0.87	0.01101	0.75
1,1,2,2-Tetrachloroethane	3.68E-05	0.98	4.98E-05	0.75	4.36E-05	0.75	4.68E-05	0.98
Chlorobenzene	3.89E-04	0.82	0.20706	0.46	0.14316	0.88	0.20986	0.72
Ethylbenzene	0.00177	0.98	1.30557	0.71	4.81392	0.75	2.28153	0.77
p-Xylene & m-Xylene	0.00379	0.89	0.70714	0.72	1.4602	0.74	9.54957	0.75
Bromoform	3.28E-05	0.85	6.73E-05	0.77	7.66E-05	0.93	7.23E-05	0.99
Styrene	0.03164	0.82	0.01236	0.79	0.2399	0.92	0.05262	0.54
o-Xylene	0.00385	0.77	0.09429	0.59	3.86706	0.54	0.64964	0.66
1,2,3-Trichloro-propane	3.69E-05	0.84	5.39E-05	0.67	3.98E-05	0.93	4.17E-05	0.97
Isopropyl benzene	0.0013	0.79	0.32989	0.58	1.24914	0.88	0.05828	0.67
Bromobenzene	6.05E-04	0.92	0.00461	0.73	0.0255	0.77	0.01077	0.70
n-Propylbenzene	0.00157	0.97	0.14126	0.72	0.53487	0.70	1.02192	0.74
2-Chlorotoluene	0.00216	0.91	0.17693	0.77	0.80581	0.83	0.14022	0.67
p-Chlorotoluene	0.00238	0.88	0.60458	0.79	1.64574	0.90	0.21626	0.66
1,3,5-Trimethylbenzene	0.00451	0.86	0.40963	0.75	3.18234	0.85	0.52274	0.66
tert-Butylbenzene	0.00109	0.84	0.80696	0.83	0.12887	0.91	0.03787	0.68
1,2,4-Trimethylbenzene	0.00386	0.93	0.38644	0.71	0.01541	0.67	0.46017	0.04
p-Propyl-toluene	0.0011	0.85	0.13051	0.83	1.02119	0.63	1.21124	0.72
1,4-Dichlorobenzene	1.62E-04	0.93	0.0071	0.74	0.02148	0.75	0.01095	0.75
1,3-Dichlorobenzene	3.25E-04	0.97	0.06471	0.75	0.39651	0.74	0.13971	0.72
p-Isopropyltoluene	0.00186	0.98	0.01372	0.72	0.00996	0.72	0.02788	0.92
1,2-Dichlorobenzene	1.74E-04	0.91	0.00754	0.94	0.02682	0.74	0.01304	0.75
n-Butylbenzene	0.00162	0.97	0.0991	0.76	0.19198	0.74	0.36456	0.79
1,2-Dibromo-3-chloro-propane	4.13E-05	0.92	7.02E-05	0.79	5.43E-05	0.90	5.51E-05	0.97
1,2,4-Trichlorobenzene	2.00E-04	0.82	0.00458	0.50	0.01388	0.96	0.00944	0.76
Naphthalene	5.56E-04	0.96	0.00667	0.80	0.00358	0.76	0.34823	0.66
Hexachlorobutadiene	2.50E-05	0.98	3.87E-05	0.52	4.43E-05	0.78	6.02E-05	0.98
1,2,3-Trichlorobenzene	6.52E-05	0.91	3.28E-04	0.96	4.59E-04	0.98	3.12E-04	0.94

Note: For those compounds with extraordinary low degradation rate, the regression coefficient could be less than 0.5 due to the experimental error.

Table 7
Variable selection results based on the GA-MLR technique

No	MLR model	Training set			Test set	
		R^2	rms	F	R^2	rms
1	$f(E_{\text{HOMO}})$	0.741	0.798	197.14	0.769	0.371
2	$f(E_{\text{HOMO}}, Q_{\text{c}}^-)$	0.763	0.795	100.16	0.749	0.481
3	$f(E_{\text{HOMO}}, Q_{\text{c}}^-, \text{DBE})$	0.770	0.784	69.23	0.748	0.483
4	$f(E_{\text{HOMO}}, Q_{\text{c}}^-, Q_{\text{h}}^+, R)$	0.693	0.789	51.50	0.737	0.474

QSAR models for the prediction of chemical toxicity, drug activity, and biodegradation of organic matters [29,30,44,45]. HOMO is the orbital that could act as an electron donor, since it is the outermost (highest energy) orbital containing electrons. A high value of E_{HOMO} indicates that the electrons are very active, increasing the electron giving ability of organic compounds, and consequently accelerating the degradation process [45]. Thus, the organic compounds are more easily attacked by radicals and appear higher reaction rates during the process of degradation. Therefore, E_{HOMO} is an appropriate indicator to predict and assess the difficulty level of VOC degradation by radicals.

Q_{c}^- is the largest negative net charge on a carbon atom. The carbon atom with higher negative net charge may have greater intermolecular electrostatic attractive interactions with the hydrogen atoms, which inhibits the abstract hydrogen reaction with radicals. Therefore, higher Q_{c}^- decreases the degradation rate constants of VOCs.

DBE, also called degree of unsaturation, helps to determine the number of rings, double bonds, and triple bonds present in a compound [46]. The compounds with high DBE are easily attacked by radicals, and have higher degradation rates. Therefore, positive correlation is expected between the logarithm of degradation rate constants $\text{Log } k$ and DBE.

The relationship between experimental and predicted rate constants is plotted in Fig. 1. In general, the reaction rates obtained from the batch experiments agreed well with the QSAR model prediction. The highest deviations from experimental data were observed for two compounds, which are naphthalene and hexachlorobutadiene (marked as black filled circles). A possible reason for naphthalene and hexachlorobutadiene as outliers is that some relevant structure feature of these two compounds was not incorporated in the current model [30]. The QSAR model plot of experimental and predicted $-\log k$ (Fig. 1) also shows that, 51 VOCs could generally be divided into three groups, illustrating the different

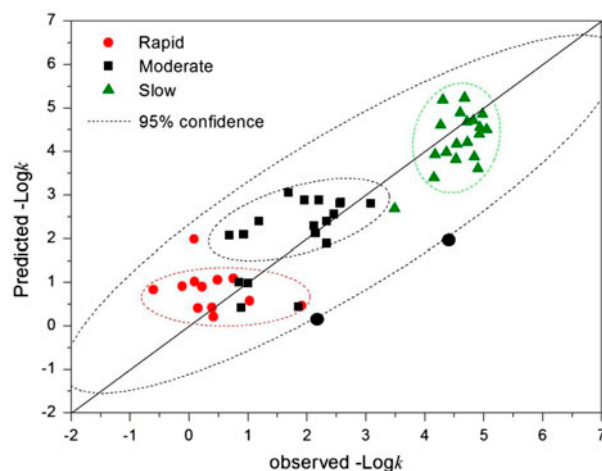


Fig. 1. Plot of experimental and predicted $-\text{Log } k$ for the data-set from VOCs degradation by SPS-Fe(II).

degradation rates of VOCs. Red, black, and green circles represent the rapid group, moderate group, and slow group separately. The classification of three groups comes from the cluster analysis performed in the following section.

3.4. Cluster analysis of VOCs

Cluster analysis has been proved to be a good exploratory data analysis method. QSAR analysis revealed that E_{HOMO} has a major contribution to QSAR model. Based on all the degradation data-set by four activated methods and E_{HOMO} , hierarchical cluster analysis (HCA) was further applied by SPSS software, and hierarchical cluster graph was given, as shown in Fig. 2.

United States Environmental Protection Agency classifies the atmospheric organic matter degradation by the radicals into four classes—rapid (<2 h), moderate (2 h–1 d), slow (1–10 d), and negligible (>10 d) [47]. Based on degradation rates and HOMO level energy of VOCs compounds, clustering method was used to

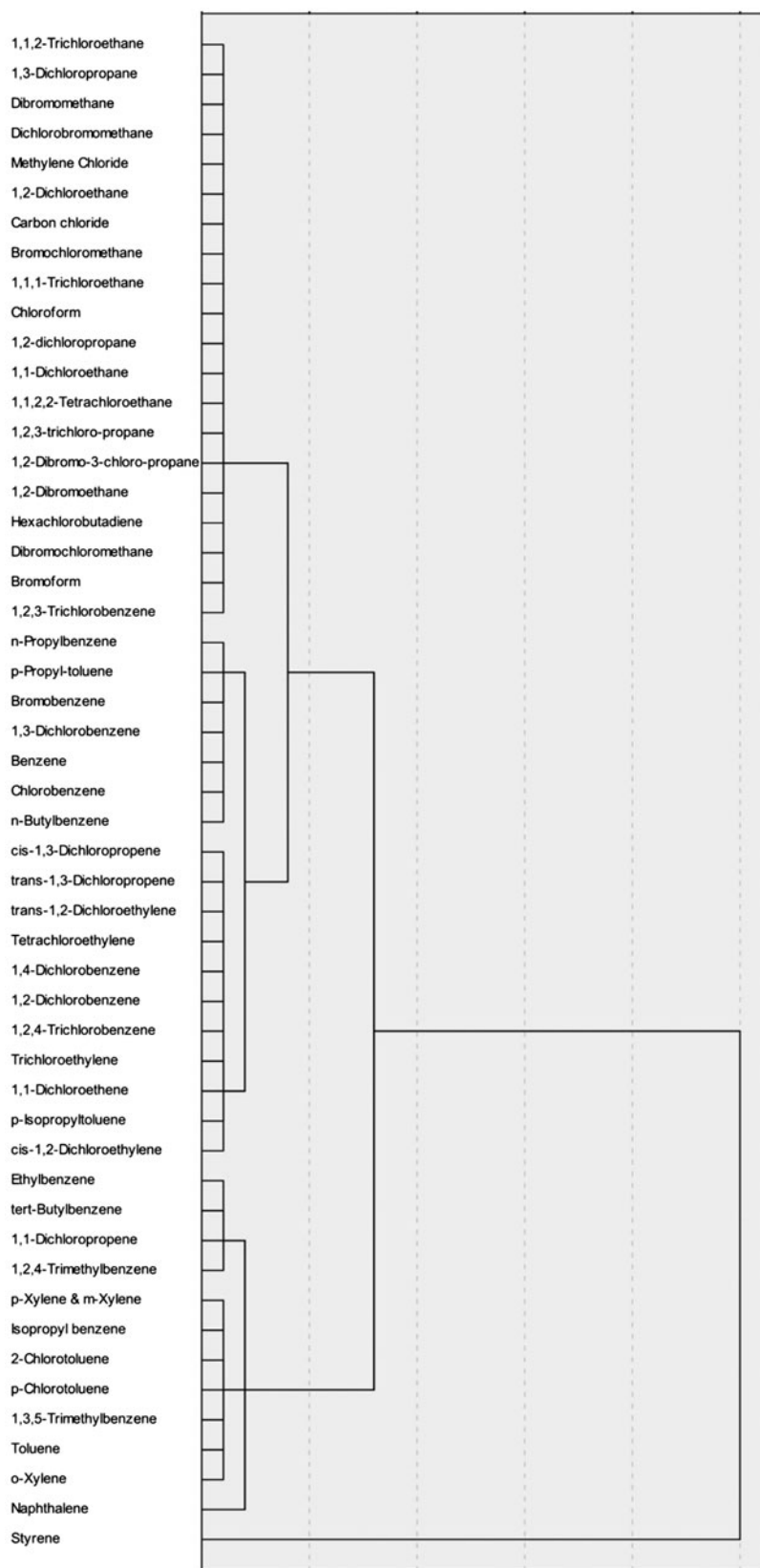


Fig. 2. HCA of VOCs compounds.

Table 8

The estimated and classification of 51 VOCs organic compounds

Classification	Number	%
Rapid	13	25.5
Moderate	18	35.3
Slow	20	39.2

classify the tested compounds into three classes—rapid, moderate, and slow. Among the 51 VOCs, 13 VOCs are classified as rapid, 18 belong to moderate and 20 fell into slow, as shown in Table 8.

The division of VOCs in QSAR model plot (Fig. 1) is similar to the three classes classified by cluster analysis (Fig. 2). However, there is slight difference between the two classifications of VOCs. For example, cluster analysis shows that *n*-butylbenzene and 4-propyltoluene are categorized to moderate group, while both compounds seems to be more easily degraded in Fig. 1 (see black points in red dash-lined eclipse). The main reason is that cluster analysis was performed using all the degradation data-set, while QSAR model (Fig. 1) only covered the data-set of VOC degradation by SPS-Fe(II), indicating the differences of degradability under varied activation conditions.

Monocyclic aromatic hydrocarbons such as ethylbenzene, toluene, and xylene are the dominant chemicals in class rapid, while several halogenated benzenes, 1,1-dichloropropene, and naphthalene are also included. Members of class rapid appear very amenable to persulfate oxidation. The results are in agreement with previous findings that BTEX (benzene, toluene, ethylbenzene, and xylene) and many monocyclic aromatic hydrocarbons were highly degradable and tended to degrade at faster rates than chlorinated benzenes [13,22,48]. Styrene is the most easily degradable organic compound in class rapid, since the unsaturated bond on the phenyl ring increased its vulnerability to radicals. The removal of styrene in 6 h by SPS alone is 41.2%, and was improved up to 95.5% under ferrous activation.

Class moderate consists of 18 VOCs. Halogenated aromatics and halogenated alkenes are the dominant compounds in this class. Previous studies indicated that halogenated aromatics could be degraded by SPS oxidation [49,50]. Luo et al. [50] showed that thermally activated persulfate could oxidize monochlorobenzene in aqueous solutions. Waldemer et al. [51] studied the degradation of PCE, TCE, *cis*-DCE, and *trans*-DCE with heat-activated persulfate and found all these chlorinated ethenes could degrade completely with persulfate. In general, halogenated aromatic

compounds, including chlorobenzene and dichlorobenzene, are slightly more difficult to be degraded than the non-halogenated counterparts, due to the inductive effect associated with the halogen atoms which results in the reduction of electron density. In contrast, the alkyl group of non-halogenated compounds could introduce hyperconjugation effect, thus facilitate the proton abstraction reaction by sulfate radicals [52].

Trihalide and quadri-halide alkanes are the dominant compounds in class slow. Compared with halogenated alkenes, halogenated alkanes tend to be much more recalcitrant to oxidation by SPS [13,53]. However, several researchers [21,49] proposed that degradation of some chlorinated methanes and ethanes by activated persulfate is still possible. The number of halogen atom in a chemical structure significantly affects the reactivity of VOCs—the larger the number of halogen atom, the lower reaction rate of organic compound with radicals, as the halogen atoms makes the benzene ring less electronically rich. For example, the reaction rate of *p*-chlorotoluene, 1,2-dichlorobenzene, and 1,2,3-trichlorobenzene under SPS alone is 0.0024, 0.00017, and 0.00006 L $\mu\text{g}^{-1} \text{h}^{-1}$, respectively.

4. Conclusion

In this study, the oxidation of 51 VOCs by SPS with or without ferrous ion activation was investigated. Four groups of VOCs treatment were studied. Without activation, 16 VOCs had a percentage of degradation over 90%, where 31 VOCs degraded over 90% under Fe(II)-activated SPS oxidation. Chelating iron Fe(II)-CA and Fe(II)-EDTA were proved to be better activators, which indicated chelating agents could increase the stability and solubility of ferrous ion at neutral pH, and control the concentration of free ferrous ion.

A GA-MLR was applied to select the descriptors to build QSAR model. The main contribution to the degradation rate was given by E_{HOMO} , DBE, and Q_c^- . Based on cluster analysis of degradation rates and main descriptors, the degradability of target VOCs were classified into three classes—rapid, moderate, and slow. The obtained statistically robust QSAR model can be used for the assessment of VOC removal by persulfate radicals as a part of environmental control technology.

Acknowledgments

The research was supported by National High Technology Research and Development Program of

China (2013AA06A608), Jiangsu Province Environmental Protection Program (2012037), Central Public-interest Scientific Institution Basal Research Fund (2014), MOHRSS Research Fund for Returned Oversea Scholars, and SEMPC Key Lab Fund (2014). The chemical calculations and software services were supported by the Supercomputing Center of Chinese Academy of Sciences, and High Performance Computing Cluster System of Changzhou University.

References

- [1] USEPA and PRC Environmental Management Inc., Roadmap to Understanding Innovative Technology Options for Brownfields Investigation and Cleanup, USEPA, Washington, DC, 1998.
- [2] E. Ferrarese, G. Andreottola, I.A. Oprea, Remediation of PAH-contaminated sediments by chemical oxidation, *J. Hazard. Mater.* 152 (2008) 128–139.
- [3] S.H. Liang, C.M. Kao, Y.C. Kuo, K.F. Chen, B.M. Yang, In situ oxidation of petroleum-hydrocarbon contaminated groundwater using passive ISCO system, *Water Res.* 45 (2011) 2496–2506.
- [4] Y. Yukselen-Aksoy, A.P. Khodadoust, K.R. Reddy, Destruction of PCB 44 in spiked subsurface soils using activated persulfate oxidation, *Water Air Soil Pollut.* 209 (2009) 419–427.
- [5] D. Zhao, X. Liao, X. Yan, S.G. Huling, T. Chai, H. Tao, Effect and mechanism of persulfate activated by different methods for PAHs removal in soil, *J. Hazard. Mater.* 254–255 (2013) 228–235.
- [6] A. Tsitonaki, B. Petri, M. Crimi, H. Mosbæk, R.L. Siegrist, P.L. Bjerg, In situ chemical oxidation of contaminated soil and groundwater using persulfate: A review, *Crit. Rev. Env. Sci. Technol.* 40 (2010) 55–91.
- [7] S.G. Huling, B.E. Pivetz, In-situ chemical oxidation, DTIC Document, Ada, Oklahoma, 2006.
- [8] A. Tsitonaki, B.F. Smets, P.L. Bjerg, Effects of heat-activated persulfate oxidation on soil microorganisms, *Water Res.* 42 (2008) 1013–1022.
- [9] D.A. House, Kinetics and mechanism of oxidations by peroxydisulfate, *Chem. Rev.* 62 (1962) 185–203.
- [10] I. Kolthoff, I. Miller, The chemistry of persulfate. I. The kinetics and mechanism of the decomposition of the persulfate ion in aqueous medium, *J. Am. Chem. Soc.* 73 (1951) 3055–3059.
- [11] W.M. Latimer, The Oxidation States of the Elements and their Potentials in Aqueous Solutions, Prentice-Hall Inc, New York, NY, 1938.
- [12] K.C. Huang, R.A. Couttenye, G.E. Hoag, Kinetics of heat-assisted persulfate oxidation of methyl tert-butyl ether (MTBE), *Chemosphere* 49 (2002) 413–420.
- [13] K.C. Huang, Z. Zhao, G.E. Hoag, A. Dahmani, P.A. Block, Degradation of volatile organic compounds with thermally activated persulfate oxidation, *Chemosphere* 61 (2005) 551–560.
- [14] X. Xie, Y. Zhang, W. Huang, S. Huang, Degradation kinetics and mechanism of aniline by heat-assisted persulfate oxidation, *J. Environ. Sci.* 24 (2012) 821–826.
- [15] G.P. Anipsitakis, D.D. Dionysiou, Radical generation by the interaction of transition metals with common oxidants, *Environ. Sci. Technol.* 38 (2004) 3705–3712.
- [16] C. Liang, C.J. Bruell, M.C. Marley, K.L. Sperry, Persulfate oxidation for in situ remediation of TCE. I. Activated by ferrous ion with and without a persulfate-thiosulfate redox couple, *Chemosphere* 55 (2004) 1213–1223.
- [17] C. Liang, I.L. Lee, I.Y. Hsu, C.P. Liang, Y.L. Lin, Persulfate oxidation of trichloroethylene with and without iron activation in porous media, *Chemosphere* 70 (2008) 426–435.
- [18] C.S. Liu, K. Shih, C.X. Sun, F. Wang, Oxidative degradation of propachlor by ferrous and copper ion activated persulfate, *Sci. Total Environ.* 416 (2012) 507–512.
- [19] M. Usman, P. Faure, C. Ruby, K. Hanna, Application of magnetite-activated persulfate oxidation for the degradation of PAHs in contaminated soils, *Chemosphere* 87 (2012) 234–240.
- [20] O.S. Furman, A.L. Teel, R.J. Watts, Mechanism of base activation of persulfate, *Environ. Sci. Technol.* 44 (2010) 6423–6428.
- [21] M. Marchesi, N.R. Thomson, R. Aravena, K.S. Sra, N. Otero, A. Soler, Carbon isotope fractionation of 1, 1, 1-trichloroethane during base-catalyzed persulfate treatment, *J. Hazard. Mater.* 260 (2013) 61–66.
- [22] M.L. Crimi, J. Taylor, Experimental evaluation of catalyzed hydrogen peroxide and sodium persulfate for destruction of BTEX contaminants, *Soil Sediment Contam.* 16 (2007) 29–45.
- [23] J. Fordham, H.L. Williams, The persulfate-iron (II) initiator system for free radical polymerizations, *J. Am. Chem. Soc.* 73 (1951) 4855–4859.
- [24] C. Liang, C.J. Bruell, M.C. Marley, K.L. Sperry, Persulfate oxidation for in situ remediation of TCE. II. Activated by chelated ferrous ion, *Chemosphere* 55 (2004) 1225–1233.
- [25] C. Liang, C.F. Huang, Y.J. Chen, Potential for activated persulfate degradation of BTEX contamination, *Water Res.* 42 (2008) 4091–4100.
- [26] C.G. Niu, Y. Wang, X.G. Zhang, G.M. Zeng, D.W. Huang, M. Ruan, X.W. Li, Decolorization of an azo dye Orange G in microbial fuel cells using Fe(II)-EDTA catalyzed persulfate, *Bioresour. Technol.* 126 (2012) 101–106.
- [27] D.Y.S. Yan, I.M.C. Lo, Removal effectiveness and mechanisms of naphthalene and heavy metals from artificially contaminated soil by iron chelate-activated persulfate, *Environ. Pollut.* 178 (2013) 15–22.
- [28] F. Nadim, K.C. Huang, A.M. Dahmani, Remediation of soil and ground water contaminated with PAH using heat and Fe(II)-EDTA catalyzed persulfate oxidation, *Water Air Soil Pollut.: Focus* 6 (2006) 227–232.
- [29] X. Yu, B. Yi, X. Wang, J. Chen, Predicting reaction rate constants of ozone with organic compounds from radical structures, *Atmos. Environ.* 51 (2012) 124–130.
- [30] H. Kušić, B. Rasulev, D. Leszczynska, J. Leszczynski, N. Koprivanac, Prediction of rate constants for radical degradation of aromatic pollutants in water matrix: A QSAR study, *Chemosphere* 75 (2009) 1128–1134.
- [31] Y. Ruiz-Morales, HOMO-LUMO gap as an index of molecular size and structure for polycyclic aromatic hydrocarbons (PAHs) and asphaltenes: A theoretical study. I, *J. Phys. Chem. A* 106 (2002) 11283–11308.

- [32] H.Y. Zhang, C. De Zhan, Is HOMO energy level a good parameter to characterize antioxidant activity, *Chin. Chem. Lett.* 11 (2000) 727–730.
- [33] P. Gramatica, P. Pilutti, E. Papa, A tool for the assessment of VOC degradability by tropospheric oxidants starting from chemical structure, *Atmos. Environ.* 38 (2004) 6167–6175.
- [34] P. Gramatica, P. Pilutti, E. Papa, Validated QSAR prediction of OH tropospheric degradation of VOCs: Splitting into training-test sets and consensus modeling, *J. Chem. Inf. Model.* 44 (2004) 1794–1802.
- [35] E. Papa, P. Gramatica, Externally validated QSPR modelling of VOC tropospheric oxidation by NO₃ radicals, *SAR QSAR Environ. Res.* 19 (2008) 655–668.
- [36] P. Pré, F. Delage, C. Faur-Brasquet, P. Le Cloirec, Quantitative structure–activity relationships for the prediction of VOCs adsorption and desorption energies onto activated carbon, *Fuel Process. Technol.* 77–78 (2002) 345–351.
- [37] K. Price, K. Krishnan, An integrated QSAR–PBPK modelling approach for predicting the inhalation toxicokinetics of mixtures of volatile organic chemicals in the rat, *SAR QSAR Environ. Res.* 22 (2011) 107–128.
- [38] M.J. Frisch, G.W. Trucks, H.B. Schlegel, G.E. Scuseria, M.A. Robb, J.R. Cheeseman, G. Scalmani, V. Barone, B. Mennucci, G.A. Petersson, H. Nakatsuji, M. Caricato, X. Li, H.P. Hratchian, A.F. Izmaylov, J. Bloino, G. Zheng, J.L. Sonnenberg, M. Hada, M. Ehara, K. Toyota, R. Fukuda, J. Hasegawa, M. Ishida, T. Nakajima, Y. Honda, O. Kitao, H. Nakai, T. Vreven, J.A. Montgomery Jr., J.E. Peralta, F. Ogliaro, M. Bearpark, J.J. Heyd, E. Brothers, K.N. Kudin, V.N. Staroverov, R. Kobayashi, J. Normand, K. Raghavachari, A. Rendell, J.C. Burant, S.S. Iyengar, J. Tomasi, M. Cossi, N. Rega, J.M. Millam, M. Klene, J.E. Knox, J.B. Cross, V. Bakken, C. Adamo, J. Jaramillo, R. Gomperts, R.E. Stratmann, O. Yazyev, A.J. Austin, R. Cammi, C. Pomelli, J.W. Ochterski, R.L. Martin, K. Morokuma, V.G. Zakrzewski, G.A. Voth, P. Salvador, J.J. Dannenberg, S. Dapprich, A.D. Daniels, Ö. Farkas, J.B. Foresman, J.V. Ortiz, J. Cioslowski, D.J. Fox, *Gaussian 09*, Revision D.01, Gaussian, Inc., Wallingford, CT, 2009.
- [39] D.B. de Oliveira, A.C. Gaudio, BuildQSAR: A new computer program for QSAR analysis, *Quant. Struct.-Act. Relat.* 19 (2000) 599–601.
- [40] F. Ballante, R. Ragno, 3-D QSAutogrid/R: An alternative procedure to build 3-D QSAR models. Methodologies and applications, *J. Chem. Inf. Model.* 52 (2012) 1674–1685.
- [41] X. Huang, X. Yu, B. Yi, S. Zhang, Prediction of rate constants for the reactions of alkanes with the hydroxyl radicals, *J. Atmos. Chem.* 69 (2012) 201–213.
- [42] X. He, A.A. de la Cruz, D.D. Dionysiou, Destruction of cyanobacterial toxin cylindrospermopsin by hydroxyl radicals and sulfate radicals using UV-254nm activation of hydrogen peroxide, persulfate and peroxymonosulfate, *J. Photochem. Photobiol., A* 251 (2013) 160–166.
- [43] H. Li, J. Wan, Y. Ma, Y. Wang, M. Huang, Influence of particle size of zero-valent iron and dissolved silica on the reactivity of activated persulfate for degradation of acid orange 7, *Chem. Eng. J.* 237 (2014) 487–496.
- [44] L. Jia, Z. Shen, W. Guo, Y. Zhang, H. Zhu, W. Ji, M. Fan, QSAR models for oxidative degradation of organic pollutants in the Fenton process, *J. Taiwan. Inst. Chem. Eng.* (2014) 140–147.
- [45] M. Karelson, V.S. Lobanov, A.R. Katritzky, Quantum-chemical descriptors in QSAR/QSPR studies, *Chem. Rev.* 96 (1996) 1027–1044.
- [46] S. Sudhakaran, G.L. Amy, QSAR models for oxidation of organic micropollutants in water based on ozone and hydroxyl radical rate constants and their chemical classification, *Water Res.* 47 (2013) 1111–1122.
- [47] USEPA, Pollution Prevention (P2) Framework, The Office of Pollution Prevention and Toxics, Washington, DC, 2005.
- [48] J. Lemaire, V. Croze, J. Maier, M.O. Simonnot, Is it possible to remediate a BTEX contaminated chalky aquifer by in situ chemical oxidation? *Chemosphere* 84 (2011) 1181–1187.
- [49] P.A. Block, R.A. Brown, D. Robinson, Novel activation technologies for sodium persulfate in situ chemical oxidation, in: *Proceedings of the Fourth International Conference on the remediation of chlorinated and recalcitrant compounds*, Monterey, California, May 24–27, 2004.
- [50] Q. Luo, Oxidative treatment of aqueous monochlorobenzene with thermally-activated persulfate, *Front. Environ. Sci. Eng.* 8 (2014) 188–194.
- [51] R.H. Waldemer, P.G. Tratnyek, R.L. Johnson, J.T. Nurmi, Oxidation of chlorinated ethenes by heat-activated persulfate: Kinetics and products, *Environ. Sci. Technol.* 41 (2007) 1010–1015.
- [52] I. McKenzie, E. Roduner, Using polarized muons as ultrasensitive spin labels in free radical chemistry, *Naturwissenschaften* 96 (2009) 873–887.
- [53] C.J. Liang, C.J. Bruell, M.C. Marley, K.L. Sperry, Thermally activated persulfate oxidation of trichloroethylene (TCE) and 1, 1, 1-trichloroethane (TCA) in aqueous systems and soil slurries, *Quant. Struct.-Act. Relat.* 12 (2003) 207–228.